

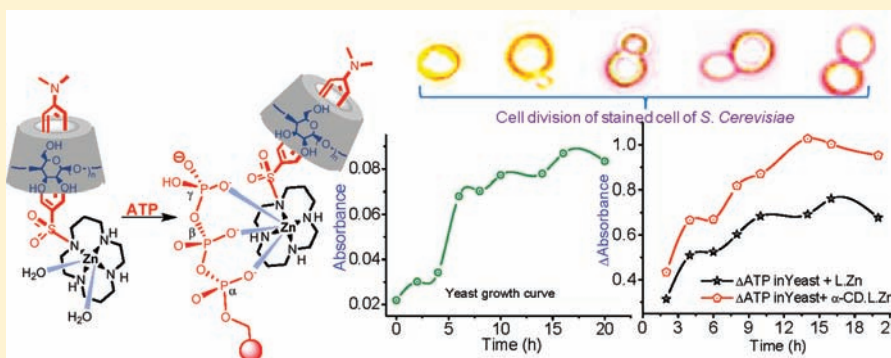
# Zn(II)–Cyclam Based Chromogenic Sensors for Recognition of ATP in Aqueous Solution Under Physiological Conditions and Their Application as Viable Staining Agents for Microorganism

Prasenjit Mahato, Amrita Ghosh, Sanjiv K. Mishra, Anupama Shrivastav, Sandhya Mishra,\* and Amitava Das\*

Central Salt & Marine Chemicals Research Institute (CSIR), Bhavnagar, 364002 Gujarat, India

Supporting Information

## ABSTRACT:



Two chromogenic complexes, **L.Zn** (where **L** is (*E*)-4-((4-(1,4,8,11-tetraazacyclotetradecan-1-ylsulfonyl)phenyl)diazenyl)-*N,N*-dimethylaniline) and its [2]pseudorotaxane form ( **$\alpha$ -CD.L.Zn**), were found to bind preferentially to adenosine triphosphate (ATP), among all other common anions and biologically important phosphate (AMP, ADP, pyrophosphate, and phosphate) ions in aqueous HEPES buffer medium of pH 7.2. Studies with live cell cultures of prokaryotic microbes revealed that binding of these two reagents to intercellular ATP, produced in situ, could be used in delineating the Gram-positive and the Gram-negative bacteria. More importantly, these dyes were found to be nontoxic to living microbes (eukaryotes and prokaryotes) and could be used for studying the cell growth dynamics. Binding to these two viable staining agents to intercellular ATP was also confirmed by spectroscopic studies on cell growth in the presence of different respiratory inhibitors that influence the intercellular ATP generation.

## INTRODUCTION

The realization that the tailor-made small molecule could be used as a selective and efficient probe for recognition of certain ionic and neutral species, having detrimental effect(s) on human health and environment, has led to a recent exponential growth in the area of molecular sensors.<sup>1,2</sup> Among different types of sensor molecules, research on the fluorescence-based chemosensors has received more attention, as these generally offer a lower detection limit for the desired analyte, as well as for their application potential in imaging processes.<sup>3</sup> This led to adverse growth for small-molecule colorimetric chemosensors; however, colorimetric or spectroscopic detection of biologically important ions and, thus, the evaluation of various biological phenomena have received considerable attention in recent years due to the obvious ease in the detection procedure.<sup>4</sup> Further, a colorimetric sensor offers the possibility of the semiquantitative visual detection of the targeted analyte(s).<sup>5</sup> Among different ions that have biological significance, recognition of anionic analytes is generally more challenging as compared to their cationic counterparts due to the high solvation energy of these anions in aqueous

medium<sup>6</sup> (pH  $\sim$  7.2) and, in some cases, a limited pH range existence.<sup>7</sup> Recognition of phosphate ions in an aqueous medium is adversely affected for such reasons. However, recognition of inorganic phosphates ( $\text{PO}_4^{3-}$  and its different protonated form, pyrophosphate ( $\text{P}_2\text{O}_7^{4-}$ ), etc.) and phosphates that are the part of respective metabolites like adenosine monophosphate (AMP), adenosine diphosphate (ADP), and adenosine triphosphate (ATP) is imperative due to their involvement in numerous crucial biological processes ranging from intercellular energy conversion and storage and metabolism to biosynthesis, signal transduction, ion-channel regulation, muscle contraction, gene regulation, etc.<sup>8</sup> ATP also serves as a phosphate donor in kinase catalyzed protein phosphorylation. ATP is present in all metabolically active cells, and its concentration gets reduced when a cell undergoes necrosis or apoptosis.<sup>9</sup> Deficiency in ATP results in ischemia, Parkinson's disease, and hypoglycemia.<sup>10</sup> Thus, monitoring the ATP concentration level is crucial for the study

Received: February 2, 2011

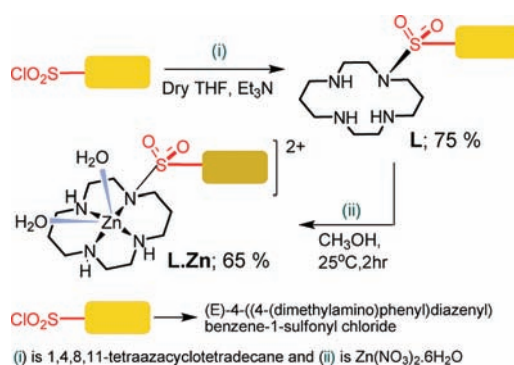
Published: March 30, 2011

of different cellular mechanisms, enzymatic processes, and cell apoptosis, as well as for assessing cytotoxic, cytostatic, and proliferative effects of drugs and biological response modifiers.<sup>11</sup> All these have necessitated the development of an appropriate reagent for rapid and convenient determination system for ATP; these include a luciferin–luciferase bioluminescence assay<sup>12,13</sup> and electrochemical,<sup>14</sup> fluorometric,<sup>6d,15</sup> and colorimetric<sup>16,17</sup> sensors. Among these, for the reasons mentioned above, research efforts for the development of chromogenic sensors that allow visual detection of ATP in physiological condition have been intensified in recent times. Despite widespread interest and recent advances, there are only a few examples of colorimetric sensors for ATP with desired sensitivity and rapid response time, which promise real-time detection of ATP under various biological conditions without special skills or instruments.<sup>17</sup> In our earlier communications,<sup>17b,c</sup> we have shown that a Zn(II)–dipicolylamine based coordination complex with a pendant azo-functionality as the reporter group could be used for staining yeast cells (*Saccharomyces cerevisiae*, an eukaryotic microbe) or in prokaryotic microbes like *Bacillus megaterium* (Gram-positive) and *Pseudomonas fluorescense* (Gram-negative) through preferential binding to the ATP produced in situ, while time duration for the staining process was about 5 min. More importantly, this reagent was found to be nontoxic to the living cells, an ideal criterion for practical applications. However, this Zn(II)-based reagent had a limited solubility in pure aqueous or HEPES buffer medium. More recently, we have synthesized a new Zn(II)–cyclam complex and reported our preliminary observations on ATP-recognition and cell viability studies using live cells of *Saccharomyces cerevisiae* (patent application details: 0093NF2009 [1242DEL2010], 24.05.2010).<sup>17a</sup>

In eukaryotes, most ATP is produced in chloroplasts (for plants), or in mitochondria (for both plants and animals). In prokaryotes, ATP is produced in the cell wall, as well as in the cytosol by glycolysis.<sup>18</sup> Among the prokaryotes, Gram-positive and Gram-negative bacteria have different cell wall structures and chemical composition,<sup>19</sup> and the classification is made based on the positive or negative results from Gram's staining method, which is generally a multistep process.<sup>20</sup> Therefore, it would be even more important for developing an appropriate staining agent that could effectively delineate the membrane of the smaller bacteria following a single step procedure.

Culture method is the most popular method for monitoring bacteria in various sources of fresh water, which is a time-consuming ( $\geq 24$  h) process for obtaining results, and more importantly, some viable bacteria are difficult to culture. Further, quantification and yeast viability are critical for fermentation,<sup>21</sup> medical examination,<sup>22</sup> wastewater treatment,<sup>23</sup> dental biofilm,<sup>24</sup> and bioengineering systems.<sup>25</sup> This necessitates the development of a more rapid and reliable staining method using reagents that are nontoxic to the wide varieties of live cells. In many instances, cells stained with certain fluorescent markers (e.g., 4,6-diamidino-2-phenylindole dihydrochloride (DAPI)) are nonviable.<sup>26</sup> Moreover, one of the major aspects that has received relatively less attention is the time profile action of energy-dependent processes in microbes, which would enable us to monitor the bioprocess in a rapid, easy, and accurate manner through ATP binding with the growing microbes, i.e., their correlation to growth kinetics response. In this present Article, we have addressed this specific issue using two viable staining agents, **L.Zn** and its [2]pseudorotaxane form ( $\alpha$ -CD-**L.Zn**) ( $\alpha$ -CD =  $\alpha$ -cyclodextrin) (Scheme 1), for different eukaryotic

**Scheme 1. Methodology Adopted for the Synthesis of L and L.Zn**

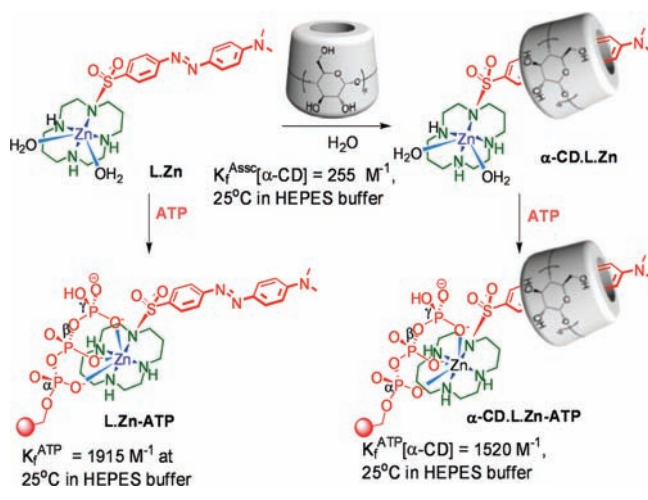


and prokaryotic cells. These reagents could even distinguish the Gram-positive (*Bacillus megaterium*) and Gram-negative (*Pseudomonas fluorescense*) bacteria following a simple one step staining procedure. Cell growth dynamics was probed by monitoring the spectral changes associated with the binding of the ATP, produced during metabolic processes of the growing microbes, to the Zn(II)-center of **L.Zn** or  $\alpha$ -CD-**L.Zn**, and this correlated well with actual cell growth kinetics response. Preliminary results on synthesis and studies on staining live cells of *Saccharomyces cerevisiae* were reported in our earlier work.<sup>17a</sup>

## RESULTS AND DISCUSSION

**Synthesis and Sensing Properties.** The intermediate ligand (E)-4-((4-(1,4,8,11-tetraazacyclotetradecan-1-ylsulfonyl)phenyl)diazenyl)-N,N-dimethylaniline (**L**) was synthesized by reacting 1,4,8,11-tetraazacyclotetradecane with (E)-4-((4-(dimethylamino)phenyl)diazenyl)benzene-1-sulfonyl chloride (Scheme 1 and Supporting Information, SI).<sup>17a</sup> Absorption maxima for **L** in  $\text{CH}_3\text{CN}/\text{CH}_2\text{Cl}_2$  (1:1, v/v) appeared at 425 nm. This charge transfer (CT) band was attributed predominantly to the  $\pi_{\text{NMe}_2}[\text{HOMO}]$ - and  $\pi_{[\text{N}=\text{N}]}^*[\text{LUMO}]$ -based transition (SI Figure 1). Systematic spectroscopic studies revealed a distinct affinity for **L** toward  $\text{Zn}^{2+}$ , and 1:1 complex formation took place in  $\text{CH}_3\text{CN}/\text{CH}_2\text{Cl}_2$  (1:1, v/v) medium with formation constant of  $3.45 \pm 0.97 \times 10^4 \text{ M}^{-1}$ ,<sup>17a</sup> while the color of the solution changed from pale yellow to pale orange. This led us to the synthesis of **L.Zn** by reacting **L** with  $\text{Zn}(\text{NO}_3)_2 \cdot 6\text{H}_2\text{O}$  in methanol medium (SI).<sup>17a</sup> Both **L** and **L.Zn** were characterized by standard analytical and spectroscopic techniques, and related spectra are provided in the Supporting Information (SI Figures 1–5). UV–vis spectra recorded for **L** and **L.Zn** (SI Figure 1) showed a broad absorption band with  $\lambda_{\text{max}}$  at 422 and at 453 nm, respectively, in  $\text{CH}_3\text{OH}-\text{CH}_3\text{CN}$  medium (3:7, v/v). This red-shifted band maximum at 453 nm for **L.Zn** was attributed to a more favored intercomponent ( $\pi-\pi^*$ ) charge transfer (CT) transition. This charge transfer nature of **L.Zn** is supported by the bathochromic shift in absorption maxima with the gradual increase in solvent polarity (SI Figure 6). This CT band for **L.Zn** in 10 mM HEPES buffer medium appeared at 463 nm. In order to examine the binding behavior of the reagent, **L.Zn**, toward various anionic analytes (e.g., ATP, CTP (cytidine triphosphate), ADP, AMP, PPi,  $\text{H}_2\text{PO}_4^-$ ,  $\text{SO}_4^{2-}$ ,  $\text{CH}_3\text{CO}_2^-$ ,  $\text{I}^-$ ,  $\text{Br}^-$ ,  $\text{Cl}^-$ ,  $\text{F}^-$ ,  $\text{CN}^-$ ,  $\text{SCN}^-$ ,  $\text{NO}_3^-$ , and  $\text{NO}_2^-$ ), UV–vis spectra for **L.Zn** were recorded in the absence and presence of

**Scheme 2. Schematic Representation of the Formation of [2]Pseudorotaxane,  $\alpha$ -CD-L.Zn, and the Binding of ATP to the Zn(II)-Center of L.Zn or  $\alpha$ -CD-L.Zn**



large excess (2000 mol equiv) of respective anions in 10 mM HEPES buffer medium (pH 7.2). A further red-shifted CT absorption band for L.Zn with a maximum at 503 nm was observed on addition of excess sodium salt of ATP (SI Figure 7). Thus, a red shift of 40 nm was achieved on binding to ATP, while an insignificant shift of 9 nm was observed when CTP of comparable concentration was added and the change for ADP was even less significant (SI Figure 7A).<sup>17a</sup> Other anionic analytes failed to induce any detectable change in electronic spectra (SI Figure 7A). A visually detectable change in solution color was also observed on addition of ATP to L.Zn solution (10 mM HEPES buffer medium), whereas this change was barely detectable for CTP and ADP. For all other anionic analytes used in this study, solution color remained unchanged. No change in spectra on addition of these anions suggests either no or a very weak binding of these anions to the Zn(II)-center of L.Zn. Systematic spectrophotometric titrations were carried out in 10 mM HEPES buffer medium in order to evaluate the relative binding affinities of ATP, CTP, and ADP toward L.Zn (SI Figures 7–9). Affinity constants for ATP ( $K_f^{[\text{L.Zn-ATP}]} = (1.9 \pm 0.15) \times 10^3 \text{ M}^{-1}$ ), CTP ( $K_f^{[\text{L.Zn-CTP}]} = (9.43 \pm 0.14) \times 10^2 \text{ M}^{-1}$ ), and ADP ( $K_f^{[\text{L.Zn-ADP}]} = (4.38 \pm 0.12) \times 10^2 \text{ M}^{-1}$ ) were evaluated under identical experimental conditions at 25 °C in aq HEPES buffer (pH of 7.2) medium using a Benesi–Hildebrand plot (SI Figure 7C and SI Figures 8 and 9). The respective binding constant for ATP, CTP, and ADP clearly reveals a highest affinity of L.Zn toward ATP. Binding constants evaluated in each case were an average of at least three independent spectrophotometric titrations. Presumably, the presence of the electron withdrawing pyrimidone functionality in CTP, as compared to the purine base in ATP, has made it a weaker electron donor, which accounts for the weaker binding of L.Zn to CTP, than that of ATP. Binding of ATP with L.Zn was also confirmed by <sup>31</sup>P NMR spectral studies. Upfield shifts were observed for the <sup>31</sup>P signals for the  $\alpha$ - (0.07 ppm),  $\beta$ - (0.09 ppm), and  $\gamma$ - (0.05 ppm) phosphorus atoms of the ATP, when bound to L.Zn.<sup>17a</sup> The shift in <sup>31</sup>P NMR signals for  $\alpha$ -,  $\beta$ -, and  $\gamma$ -P atoms signify the binding to the Zn(II)-center of L.Zn through the oxygen atom, bearing the negative charge of the respective phosphate unit. Relatively weaker interaction of the  $\text{O}_{[\gamma\text{-PO}_4]}^-$

and  $\text{O}_{[\alpha\text{-PO}_4]}^-$  compared to the  $\text{O}_{[\beta\text{-PO}_4]}^-$  unit accounts for the smaller  $\Delta\delta$  shift in <sup>31</sup>P NMR spectra. This observation also confirms the formation of a heptacoordinated Zn(II)-center in L.Zn in the presence of ATP (Scheme 2). Examples of heptacoordinated Zn(II)-centers are available in the literature.<sup>29</sup> A very insignificant shift in <sup>31</sup>P signals was observed when similar experiments were repeated for CTP, while no shift was observed for ADP for similar experiments.<sup>17a</sup> The <sup>31</sup>P NMR spectral data also confirms the affinity that was established through spectral studies (ATP  $\gg$  CTP > ADP  $\gg$  AMP). Presumably, the higher electrostatic interaction between the  $\text{Zn}^{2+}$ -center and triphosphates and the formation of a higher number of chelate rings between ATP or CTP and L.Zn are crucial for efficient L.Zn–O<sub>Phosphate</sub> binding, as compared to those for ADP and AMP. The lack of any interaction between PPi, despite having the similar “4<sup>-</sup>” charge as that of CTP/ATP, and L.Zn perhaps is better explained on the basis of its very high solvation energy.<sup>30</sup> The 1:1 complex formation (L.Zn–ATP) was further confirmed by ESI-MS spectral studies (SI Figure 10). Signals at 1103.9 and 1082 correspond to  $m/z$  for  $[\text{L.Zn-ATP}] - 2(\text{NO}_3^-)$  (A) and  $[(\text{A} - \text{Na}^+) + \text{H}^+]$ , respectively, with anticipated isotope distribution.

Reversible binding of L.Zn to ATP could be demonstrated by adding an aqueous solution of sodium citrate ( $5.0 \times 10^{-4} \text{ M}$ ) to L.Zn–ATP. The original spectrum of L.Zn (with  $\lambda_{\text{max}} = 463 \text{ nm}$ ) was restored when an aqueous solution of excess sodium citrate was added to the solution of L.Zn–ATP (SI Figure 11).

More interestingly, the solubility of the L.Zn ( $0.045 \text{ g L}^{-1}$ ) in water was found to be substantially enhanced ( $0.34 \text{ g L}^{-1}$ ) in the presence of excess  $\alpha$ -CD ( $4.5 \text{ g L}^{-1}$ ) (SI Figure 12). Favored nonbonded interactions between the (dimethylamino)phenyl)diazanyl)benzene fragment of L.Zn and the hydrophobic interior of the  $\alpha$ -CD on inclusion into the  $\alpha$ -CD cavity could account for the observed enhanced solubility of L.Zn in water; such inclusion of analogous (*E*)-1,2-di(pyridin-4-yl)ethene and (*E*)-1,2-di(pyridin-4-yl)diazene in  $\alpha$ -CD was reported earlier.<sup>31,32</sup> The absorption maximum for L.Zn (463 nm) was found to shift to shorter wavelength (458 nm) in the presence of  $\alpha$ -CD (SI Figure 13). The kinetics of such complex formation is generally ultrafast, and thus, any spectral change associated with the formation of an inclusion complex is expected to evade the normal optical spectroscopic measurements.<sup>31j</sup> Weak perturbation of the HOMO–LUMO gap absorption spectral bands<sup>31,32</sup> was anticipated for such inclusion complex formation and resulted in the 5 nm blue shift of the intercomponent ( $\pi$ – $\pi^*$ )-based CT band for L.Zn with  $\lambda_{\text{max}}$  at 458 nm (SI Figure 13). Thus, the blue shift of 5 nm could be attributed to the formation of a [2]pseudorotaxane complex,  $\alpha$ -CD.L.Zn. Presumably, formation of the more polar excited state for  $\alpha$ -CD.L.Zn is less favored in the apolar interior of  $\alpha$ -CD than in the surrounding solvent for a nonincluded reagent L.Zn.<sup>33</sup> Analogous studies were repeated with  $\beta$ -CD ( $\beta$ -cyclodextrin). Evaluation of the respective association constants from systematic spectrophotometric titration revealed a higher value for  $\alpha$ -CD.L.Zn formation than that of  $\beta$ -CD.L.Zn ( $K_f^{\text{Assoc}}(\alpha\text{-CD}) = 255 \pm 15 \text{ M}^{-1}$  and  $K_f^{\text{Assoc}}(\beta\text{-CD}) = 221 \pm 13 \text{ M}^{-1}$  at 25 °C) (SI Figure 13 and SI eq 3). However, these association constant values are close to those reported earlier for related systems.<sup>31</sup> As  $\alpha$ -CD forms a stronger inclusion complex with L.Zn, we have used  $\alpha$ -CD.L.Zn for further studies. In the presence of excess  $\alpha$ -CD (10-fold), the [2]pseudorotaxane form, i.e.,  $\alpha$ -CD.L.Zn (Scheme 2), is

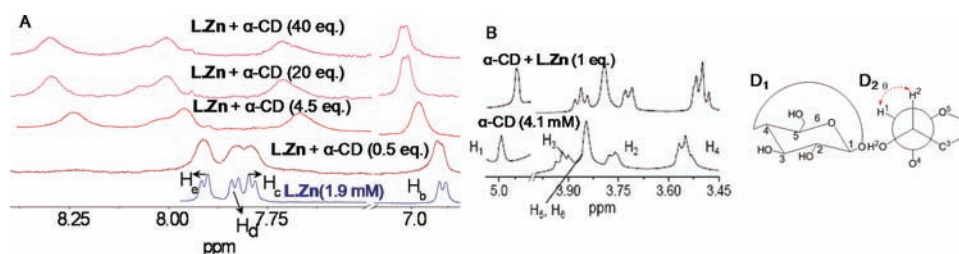


**Figure 1.** (A) Partial  $^1\text{H}$  NMR spectra of  $\text{L.Zn}$  (1.9 mM) with varying  $[\alpha\text{-CD}]$  (0–76 mM) (in  $\text{D}_2\text{O}$ ). (B)  $^1\text{H}$  NMR spectra of  $\alpha\text{-CD}$  (4.1 mM) in presence of  $\text{L.Zn}$  (1 equiv) (in  $\text{CD}_3\text{OD}/\text{D}_2\text{O} = 1:1$ ) for  $\delta = 3.45\text{--}5.04$  ppm, a region where  $\text{L.Zn}$  does not have a resonance signal. ( $\text{D}_1$  and  $\text{D}_2$ ) Schematic representation of pyranose structure and gauche conformation of  $\alpha\text{-CD}$  with  $\theta$  as the dihedral angle involving two vicinal hydrogen atoms,  $\text{H}_1$  and  $\text{H}_2$ , of the pyranose ring.

expected to be the major component ( $\geq 96\%$ ) either in the aqueous solution or in HEPES buffer. Interestingly, formation of the inclusion complex ( $\alpha\text{-CD.L.Zn}$ ) allowed for dissolving a higher amount of  $\text{L.Zn}$  in water.

We also studied the inclusion complex ( $\alpha\text{-CD.L.Zn}$ ) formation by  $^1\text{H}$  NMR spectroscopy. A gradual downfield shift for three aromatic hydrogen atoms ( $\text{H}_b$ ,  $\text{H}_d$ , and  $\text{H}_e$ ) of  $\text{L.Zn}$  (SI Scheme 1) were observed on the addition of increasing amounts of  $\alpha\text{-CD}$ , while a subsequent upfield shift for  $\text{H}_c$  of  $\text{L.Zn}$  was observed (Figure 1A). These shifts were more prominent for  $\text{H}_e$  ( $\Delta\delta = 197.5$  Hz) and  $\text{H}_d$  ( $\Delta\delta = 90.5$  Hz), respectively (Figure 1A), whereas the extent of downfield shift for  $\text{H}_b$  ( $\Delta\delta = 55$  Hz) and upfield shift for  $\text{H}_c$  ( $\Delta\delta = 33$  Hz) were relatively small. Such upfield and downfield shifts of the host protons on inclusion complex formation with  $\alpha\text{-CD}$  are not very uncommon.<sup>31n</sup>

The extent and direction of such shifts indicate a difference in the extent of shielding and deshielding interactions of the respective proton ( $\text{H}_b$ ,  $\text{H}_c$ ,  $\text{H}_d$ , and  $\text{H}_e$ ) of  $\text{L.Zn}$  (SI Scheme 1 and Figure 1) on forming the inclusion complex with  $\alpha\text{-CD.L.Zn}$  through inclusion of  $\text{L.Zn}$  in the  $\alpha\text{-CD}$  cavity. The downfield shift indicates the proximity of a hydrogen atom to an electro-negative oxygen atom, while the local polarity variation due to van der Waals' forces between the aromatic guest and cyclodextrin host could have accounted for the observed upfield shift of certain protons. Presumably, both influences are operational on each hydrogen atom of the bis(azo phenyl)-part of the guest molecule ( $\text{L.Zn}$ ), and the relative extent, as well as direction of shift, is the result of the overall influence of these two opposing effects.<sup>31n-r</sup> Upfield shifts of 25.5–54.8 Hz were also observed for the hydrogens ( $\text{H}_1\text{--H}_6$ ) of the  $\alpha\text{-CD}$  moiety (Figure 1B). Similar upfield shifts were also reported for an analogous [2]pseudorotaxane formation with 4,4'-bipyridine derivatives and  $\alpha\text{-CD}$ .<sup>31,32</sup> Presence of the shielding effect due to diamagnetic anisotropy of the benzenoid moiety of the included azo compound could account for such upfield shifts. In the present situation, after initial inclusion of  $\text{L.Zn}$  in the  $\alpha\text{-CD}$  cavity, possible polar interaction between the  $\text{--SO}_2\text{--}$  moiety of the sulphonamide fragment and  $\text{--CH}_2\text{OH}$  functionality of the  $\alpha\text{-CD}$  larger rim could induce conformational changes of the host cavity. Further support for the conformational change(s) of the host  $\alpha\text{-CD}$  cavity was available in the detailed  $^1\text{H}$  NMR studies.  $^1\text{H}$  NMR spectra of  $\alpha\text{-CD}$  (4.1 mM) and  $\alpha\text{-CD}$  in the presence of  $\text{L.Zn}$  (1 mol equiv) were recorded in  $\text{CD}_3\text{OD}/\text{D}_2\text{O}$  (1:1, v/v). A critical examination, comparison of these two  $^1\text{H}$  NMR spectra, and evaluation of the coupling constants for the interaction between vicinal  $\text{H}_1$  and  $\text{H}_2$  hydrogen of the pyranose

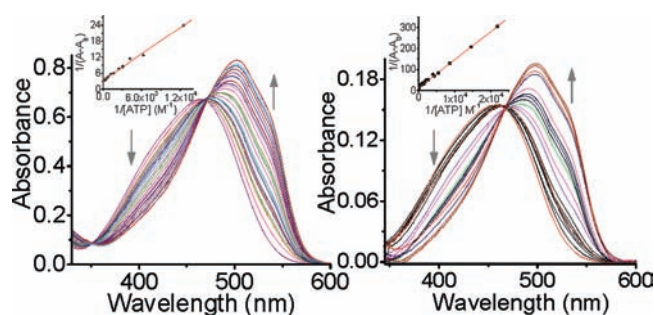


**Figure 2.** Change in absorption spectra of (A)  $\text{L.Zn}$  ( $9.46 \mu\text{M}$ ) in the presence of varying  $[\text{ATP}]$  (0–17.28 mM). (B)  $\alpha\text{-CD.L.Zn}$  ( $[\text{L.Zn}] = 2.66 \mu\text{M}$ ;  $[\alpha\text{-CD}] = 26.6 \mu\text{M}$ ) with varying  $[\text{ATP}]$  (0–0.032 M) in aq HEPES buffer (pH = 7.2). Inset: Benesi–Hildebrand plot of  $1/(A - A_0)$  vs  $1/[\text{ATP}]$  for the change in absorbance at 536 nm, upon addition of ATP to  $\text{L.Zn}/\alpha\text{-CD.L.Zn}$ .

structure suggested a definite change in the coupling constant,  $^3J_{12}$ , for the  $\alpha\text{-CD}$  moiety (Figure 1 $\text{D}_1$ ,  $\text{D}_2$  and SI Table 1). This change in coupling constant value ( $\Delta^3J_{12}$ ) can be used to calculate the change in dihedral angle ( $\Delta\theta$ ) involving two vicinal  $\text{H}_1$  and  $\text{H}_2$  atoms of the pyranose ring of the host  $\alpha\text{-CD}$  moiety on forming an inclusion complex (SI).<sup>31l</sup> Value for  $\Delta\theta = 10.6$  was thus evaluated (SI Table 1). The broadness in the observed spectra (Figure 1B) might have contributed to some inaccuracy in evaluating this calculated dihedral angle ( $\theta$ ); however, such change in  $\theta$  is reported earlier for related inclusion complexes with  $\alpha\text{-CD}$  as host.<sup>31k,l</sup>

All these results clearly indicate the formation of a host–guest inclusion complex between  $\text{L.Zn}$  and  $\alpha\text{-CD}$ . Further, the [2]pseudorotaxane formation was also confirmed by ESI-MS studies; a molecular ion peak for  $\alpha\text{-CD.L.Zn}$  was observed at  $m/z$  value of 1648.6 (SI Figure 14). More importantly, the formation of such inclusion complex helped to dissolve a higher amount of  $\text{L.Zn}$  (0.5 mM) in aqueous solution and thus resulted in a more intense color change on binding to ATP (5 mM) (*vide infra*). The binding constant for ATP to  $\text{L.Zn}$  or  $\alpha\text{-CD.L.Zn}$  was evaluated from spectroscopic titration data (Figure 2).

Systematic changes in the spectral pattern of  $\text{L.Zn}$  or  $[\alpha\text{-CD.L.Zn}]$  were recorded with increasing  $[\text{ATP}]$  in aq HEPES buffer medium (pH 7.2) and are shown in Figure 2. The absorption maximum around 457 nm was found to decrease with a concomitant increase in absorbance at 503 nm for  $\text{L.Zn}$  (isosbestic points at 420 and 466 nm) and at 499 nm for  $\alpha\text{-CD.L.Zn}$  (isosbestic point at 468 nm). Thus a red shift of 46 and 42 nm was observed on binding of ATP to the Zn(II)-center of

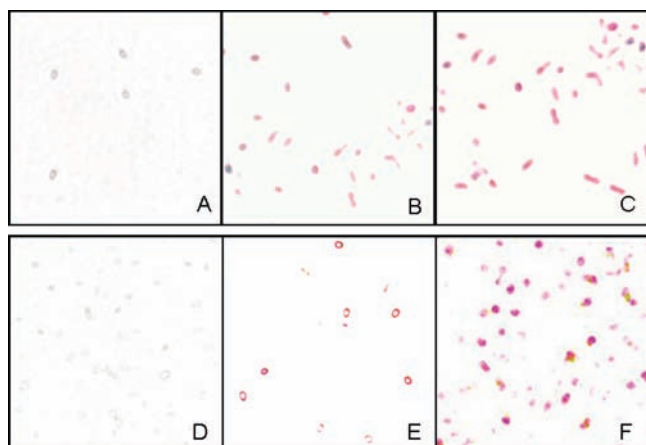


**Figure 3.** Light microscope images of Gram-positive bacteria (A) unstained and stained with (B) **L.Zn** ( $0.66 \times 10^{-4}$  M) and (C)  $\alpha$ -CD.L.Zn  $\{[\text{L.Zn}] = (5 \times 10^{-4}$  M) and  $[\alpha\text{-CD}] = (5 \times 10^{-3}$  M) $\}$  at 25 °C. Light microscope images of Gram-positive bacteria (D) unstained and stained with (E) **L.Zn** ( $0.66 \times 10^{-4}$  M) and (F)  $\alpha$ -CD.L.Zn  $\{[\text{L.Zn}] = (5 \times 10^{-4}$  M) and  $[\alpha\text{-CD}] = (5 \times 10^{-3}$  M) $\}$  at 25 °C in 10 mM HEPES buffer solution (pH = 7.2).

**L.Zn** and  $\alpha$ -CD.L.Zn, respectively. The association constants for the formation of the complex **L.Zn-ATP** and  $\alpha$ -CD.L.Zn-ATP were evaluated using Benesi–Hildebrand plot (Figure 2) and thus found to be  $K_f^{[\text{L.Zn-ATP}]} = (1.9 \pm 0.15) \times 10^3 \text{ M}^{-1}$  and  $K_f^{[\alpha\text{-CD.L.Zn-ATP}]} = (1.52 \pm 0.09) \times 10^3 \text{ M}^{-1}$ . This shows a slightly lower value for  $\alpha$ -CD.L.Zn-ATP, as compared to that for **L.Zn-ATP**. A visually detectable color change was noticed for  $\alpha$ -CD.L.Zn on binding of ATP, and this change was little more prominent than that observed for **L.Zn** under a comparable condition (SI Figure 12). Such a prominent color change was not observed when ADP or CTP was used instead of ATP for binding to  $\alpha$ -CD.L.Zn. This visual change in color for **L.Zn** and  $\alpha$ -CD.L.Zn on binding to ATP led us to explore the feasibility of using these two reagents for staining of the live eukaryote (yeast) and prokaryote (Gram-positive and Gram-negative bacteria) cells, as these microbes produce ATP in their cell surface during metabolic processes.<sup>35</sup> Preferential binding of **L.Zn** toward ATP was also established by spectroscopic studies carried out in the presence of 5 mol equiv excess of all other anions as compared to that for ATP (SI Figure 15).

**Staining Studies of the Prokaryotes (Gram-Positive and Gram-Negative Bacteria).** *Light Microscopy Image.* In our earlier studies we could demonstrate that **L.Zn** or  $\alpha$ -CD.L.Zn could be used as a colorimetric staining agent for yeast cells and the staining nature could be viewed under a simple light microscope.<sup>17a</sup> Binding of the ATP ions, produced in situ, on the cell surface to **L.Zn** or  $\alpha$ -CD.L.Zn accounted for the plausible reason for the observed staining. We have also checked the possibility of using these reagents for staining cells of *Bacillus sp.* (Gram-positive) and *Pseudomonas sp.* (Gram-negative) bacteria. Figure 3A–F revealed the images of cells of Gram-positive and Gram-negative bacteria in the absence and presence of these two reagents, when viewed under light microscope.

Figure 3B,E revealed images of the same bacteria when viewed in the presence of **L.Zn** ( $66 \mu\text{M}$ ). These images clearly showed a distinct change in color of the bacterial strain in the presence of **L.Zn**. Figure 3C,F revealed images of the same bacteria when viewed in the presence of  $\alpha$ -CD.L.Zn ( $[\text{L.Zn}] = 5 \times 10^{-4}$  M and

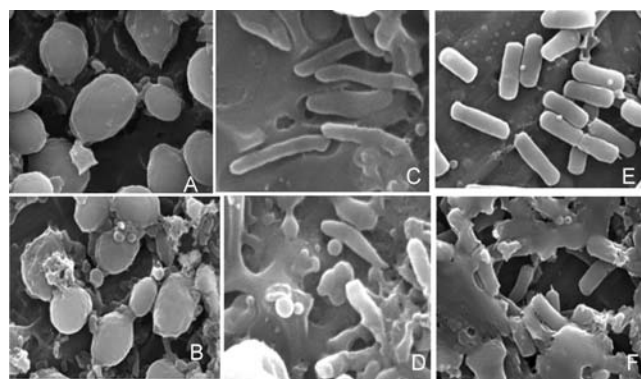


**Figure 4.** SEM images of (A) blank yeast cells, (B) yeast cells treated with **L.Zn**, (C) blank Gram-positive bacterial cells, (D) Gram-negative bacterial cells treated with **L.Zn**, (E) Gram-positive bacterial cells, and (F) Gram-negative bacterial cells treated with **L.Zn** ( $[\text{L.Zn}] = 0.66 \times 10^{-4}$  M).

$[\alpha\text{-CD}] = 5 \times 10^{-3}$  M). Figure 3B–E, taken with identical magnification, revealed that the both dyes (**L.Zn** and  $\alpha$ -CD.L.Zn) could distinguish Gram-positive and Gram-negative bacteria through distinctly different color, color intensities, and shape of the stained cells. As anticipated, stained cells for Gram-positive bacteria appeared longer in the images (Figure 3B,C), while more intense staining was observed Gram-negative bacteria (Figure 3E,F). Again after staining with **L.Zn**/ $\alpha$ -CD.L.Zn, the color of the Gram-positive bacterial cells changed from colorless to pink, whereas in the case of Gram-negative bacteria the color change occurs from colorless to violet. The difference in the staining intensity for two different bacteria could be better understood if one considers the difference in cell structure and cell wall composition of the respective bacteria. Further, the amount of extracellular ATP being released by Gram-negative bacteria is reported to be more than that of the Gram-positive bacteria, and this could contribute to the more intense staining of the Gram-negative bacteria.<sup>35</sup> The thinner, hydrophilic, and more porous cell walls of the Gram-negative bacteria are expected to allow higher excretion of ATP to the cell surface, where it gets bound to the present dye **L.Zn** or  $\alpha$ -CD.L.Zn and thereby contributes also to the more efficient staining. Existing reports on the recognition of ATP are mostly based on the changes in fluorescence or electrochemical properties,<sup>14,15</sup> and examples for the colorimetric detection of ATP in aqueous solution are rather limited.<sup>16,17</sup>

**Scanning Electron Microscopy.** SEM images (Figure 4) of blank and stained eukaryote (yeast) and prokaryote (Gram-positive and Gram-negative) cells revealed the change(s) in the morphology of the outer surface of the cells on staining. SEM images of yeast cells without dye were found to be smooth in contrast to the images of the yeast cells with dye, where stained cell surfaces were found to be rough. This signifies the presence of the extraneous material, i.e., **L.Zn**, on the cell surface. Similar changes on the cell surfaces for Gram-negative and Gram-positive bacteria in the absence and presence of staining agent, **L.Zn**, were also evident from the SEM images recorded (Figure 4C–F). The difference in the contrasts in the SEM images of the sample surfaces also signifies the nonhomogeneous chemical nature of the sample surface. Relatively brighter cell exterior for Gram-negative bacteria, as compared to the Gram-positive bacteria, indicates the accumulation of higher negative

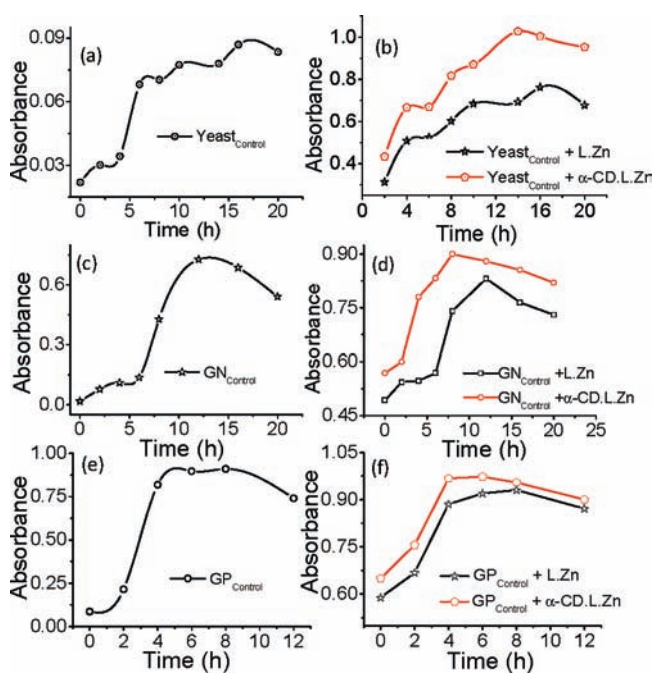


**Figure 5.** Growth curve of (a) *Saccharomyces cerevisiae*, (c) *Pseudomonas fluorescense*, and (e) *Bacillus megaterium* obtained from change in cell count with time. Relative change in absorbance at 600 nm for aqueous culture medium of (b) *Saccharomyces cerevisiae*, (d) *Pseudomonas fluorescense*, and (f) *Bacillus megaterium* in presence of 100  $\mu\text{L}$  L.Zn (0.106 mM)/ $\alpha$ -CD.L.Zn (L.Zn = 0.164 mM;  $\alpha$ -CD = 1.64 mM) in 10 mM HEPES buffer (pH = 7.2).

charge on the cell surface. Gram-negative bacteria possess a lipid-rich outer membrane (as well as a plasma membrane) and a thin peptidoglycan layer, along with a pore forming protein like porins spanning the outer surface.<sup>36</sup> All these favor a higher accumulation of the ATP at its cell surface and thereby the higher accumulation of L.Zn-ATP, which could account for the brighter exterior in the SEM image for the Gram-negative bacteria exposed to L.Zn. This also supports the more intense staining of the Gram-negative bacteria on staining with L.Zn or  $\alpha$ -CD.L.Zn and viewing through optical microscope (Figure 3).

**Viability Assay of the Cells after Staining with L.Zn Complex.** The cell division of the live yeast cells was checked before and after staining with the L.Zn or  $\alpha$ -CD.L.Zn under the light microscope over a period of 2 h after the stained cell suspension was taken as a hanging drop prepared on a concavity slide (SI Figure 16). It is worth mentioning that unstained yeast cells could not be viewed through optical microscope as these were colorless and cells appeared as yellow on staining with L.Zn and as yellow-orange on staining with  $\alpha$ -CD.L.Zn (SI Figure 16).<sup>17a</sup> In our earlier work we have reported that cell division of *Saccharomyces cerevisiae* cells remains unaffected in absence and presence of L.Zn and  $\alpha$ -CD.L.Zn.<sup>17a</sup> To develop a better understanding about the viability of these reagents, cell growth and motility for cells were checked for eukaryotic (*Saccharomyces cerevisiae*) and prokaryotic (*Bacillus megaterium* (Gram-positive) and *Pseudomonas fluorescense* (Gram-negative)) microbes. Unaffected cell proliferation confirmed that the staining agent (either L.Zn or  $\alpha$ -CD.L.Zn) was nontoxic and kept cells viable even after staining. Thus, L.Zn and  $\alpha$ -CD.L.Zn could be used as chemosensors for bioactive molecules like ATP produced in live cells through different metabolic processes and thereby can be

useful for checking the cell growth dynamics for the above referenced microbes. Results of such experiments are expected to confirm the viability of these two colorimetric staining reagents.

**Growth Curve Study.** The growth profiles of eukaryotic (*Saccharomyces cerevisiae*) and prokaryotic (Gram-negative (*Pseudomonas fluorescense*) and Gram-positive (*Bacillus megaterium*)) cells in an aqueous culture medium in the absence and presence of L.Zn and  $\alpha$ -CD.L.Zn are shown in Figure 5. Change in absorbance (at  $\lambda_{\text{max}} = 600$  nm) versus time ( $t$ ) was plotted up to 20 h, as no appreciable change in growth was observed thereafter. Figure 5a–f revealed a nice correlation between the cell growth and the ATP generation with progressive growth of the respective cells during the metabolic processes.

These kinetic studies were carried out to monitor the different phases of growth, wherein the increase in the ATP concentration as the batch culture grows from lag phase to log phase and then stationary phase was observed, and ultimately a steady decline in the growth curve was observed. Figure 5a,c,e shows the actual growth curve of live cells of *Saccharomyces cerevisiae*, *Pseudomonas fluorescense*, and *Bacillus megaterium*, respectively, with time, while Figure 5b,d,f shows a relative buildup of [ATP] in cytoplasm, measured with time for *S. cerevisiae*, *Pseudomonas fluorescense*, and *Bacillus megaterium*, respectively, at 27 °C in 10 mM aq HEPES buffer (pH = 7.2) medium. A close review of Figure 5 reveals that the actual cell growth and the relative buildup in ATP concentration, measured spectrophotometrically using reagents L.Zn and  $\alpha$ -CD.L.Zn, in the cultures under identical experimental conditions matched nicely. The relative decrease, observed in actual cell growth and ATP concentration (Figure 5), can be explained if one considers that the catabolic processes, which consume ATP, become more important after a certain time. Neither ATP nor ADP/AMP/PPi can be stored at high concentration within the cells of the living system. Their relative concentrations in cytoplasm are generally regulated over a narrow concentration limit by various biological processes. The concentration of intercellular ATP is typically around  $(1.0\text{--}10) \times 10^{-3}$  M,<sup>37</sup> and spectrophotometric measurements revealed that the lower detection limit of ATP for both these colorimetric staining agents are much lower (lower detection limits of ATP for L.Zn and  $\alpha$ -CD.L.Zn are 18 and 23  $\mu\text{M}$ , respectively) than this. Thus, kinetic studies revealed that cell growth and release of ATP during the metabolic process could be correlated using either L.Zn or  $\alpha$ -CD.L.Zn as the staining agent. Extent of absorbance changes and the higher slope observed in the case of Gram-negative bacteria revealed a higher binding of L.Zn or  $\alpha$ -CD.L.Zn to ATP released during the cell growth, as compared to that of Gram-positive.

To ascertain that L.Zn or  $\alpha$ -CD.L.Zn binds to ATP produced during metabolic processes, studies with the aqueous culture medium of the yeast cells were carried out in the absence and presence of three different respiratory inhibitors: namely, CCCP (carbonylcyanide-*m*-chlorophenylhydrazone, 100  $\mu\text{L}$  of 300  $\mu\text{g}/\text{mL}$ ),<sup>38a</sup> rotenone (100  $\mu\text{L}$  of 300  $\mu\text{g}/\text{mL}$ ),<sup>38b</sup> and cycloheximide (1  $\mu\text{L}$  of 2  $\mu\text{g}/\text{mL}$ ).<sup>38c</sup> CCCP is generally thought to increase proton permeability across the cell membrane, with consequent dissipation of the membrane potential and inhibition of ATP synthesis.<sup>39</sup> Rotenone interferes with the electron transport chain in mitochondria and thus interferes with NADH during the creation of usable cellular energy (ATP).<sup>40</sup> Thus, CCCP and rotenone are expected to inhibit the proton pump of yeast cells, and this causes the inhibition of the plasma membrane ATPase

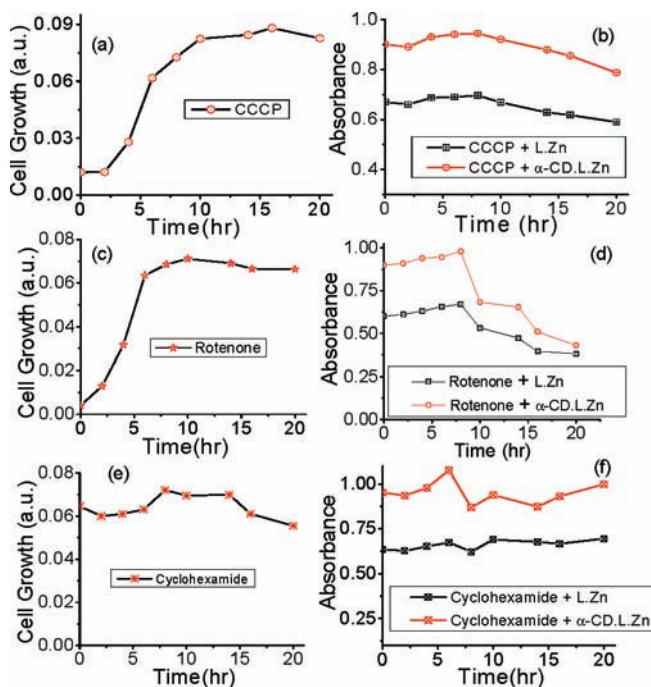


**Figure 6.** Growth curve of *Saccharomyces cerevisiae* and relative change in [ATP] with time. Change in absorbance at 600 nm for aqueous culture medium of *Saccharomyces cerevisiae* in the presence of (a) 100  $\mu\text{L}$  of 300  $\mu\text{g}/\text{mL}$  CCCP in 200 mL of culture, (c) 100  $\mu\text{L}$  of 300  $\mu\text{g}/\text{mL}$  rotenone in 200 mL of culture, (e) 1  $\mu\text{L}$  of 2  $\mu\text{g}/\text{mL}$  cycloheximide in 200 mL of culture. Relative changes in ATP concentration in the presence (control) of (b) 100  $\mu\text{L}$  L.Zn/ $\alpha$ -CD.L.Zn + 100  $\mu\text{L}$  of 300  $\mu\text{g}/\text{mL}$  CCCP, (d) 100  $\mu\text{L}$  L.Zn/ $\alpha$ -CD.L.Zn + 100  $\mu\text{L}$  of 300  $\mu\text{g}/\text{mL}$  (rotenone), (f) 100  $\mu\text{L}$  L.Zn/ $\alpha$ -CD.L.Zn + 1  $\mu\text{L}$  of 2  $\mu\text{g}/\text{mL}$  Cyh  $\{[\text{L.Zn}] = 0.106 \text{ mM}, [\alpha\text{-CD.L.Zn}] = ([\text{L.Zn}], 0.164 \text{ mM}; [\alpha\text{-CD}], 0.938 \text{ mM})$  in 10 mM HEPES buffer (pH = 7.2)}.

activity only and does not interfere with the growth of the cells. For control experiment when these were not added to the culture media of the yeast cells, growth curves remain almost unaffected (Figure 5). Cycloheximide blocks the peptidyl transferase of 80S eukaryotic ribosomes and, thus, interferes with the translocation step in protein synthesis, blocking translational elongation and inhibiting the cell growth.

Figure 6a–f clearly reveals the cell growth and ATP generation with time for yeast cells, where ATP intracellular buildup was evaluated spectrophotometrically using either L.Zn or  $\alpha$ -CD.L.Zn as the colorimetric reagent. Comparison of Figure 6a,b suggests that cell growth for *Saccharomyces cerevisiae* remained unaffected in absence or presence of CCCP, whereas comparison of Figure 6c,d suggests that cell growth for *Saccharomyces cerevisiae* remained unaffected in absence or presence of rotenone. Additionally, comparison of Figure 6a–d suggests that there was no increase in intracellular [ATP] during the lag phase of the cell growth; on the contrary a slight decrease in [ATP] was registered with time in Figure 6b,d for experiments carried out in presence of inhibitors like CCCP and rotenone, respectively. Thus, the initial ATP generation with progressive growth of the respective cells during the metabolic processes was found to be appreciably affected on addition of CCCP/rotenone to the yeast cell culture stained with L.Zn/ $\alpha$ -CD.L.Zn. This observation agrees well with the previous reports which state that CCCP/rotenone inhibits the generation of ATP.<sup>38a,b</sup> In the case of

CCCP/rotenone, a slight increase in ATP generation was observed until 8 h. Then, beyond 10 h, where the stationary phase was achieved, a gradual decrease in the ATP generation curve (Figure 6b) was registered. Due to an appreciable increase in the cell numbers up to  $\sim 10$  h (Figure 6a), concentration of CCCP was not sufficient to completely inhibit the plasma membrane ATPase activity, and a nominal increase in ATP concentration was registered until  $\sim 8$  h, after which stationary phase was attained. After stationary phase the cell numbers remain unaltered, but the ATP generation gets inhibited. For rotenone the decrease in ATP was little more prominent (Figure 6c,d). Cell growth studies on *Saccharomyces cerevisiae* in the presence of cycloheximide clearly revealed a complete inhibition of the growth of the yeast cell, as well as the ATP production (Figure 6e,f).<sup>38c</sup> Thus, these results obtained in the presence of a different respiratory inhibitor tend to confirm that the binding of ATP to the Zn(II)-center of L.Zn/ $\alpha$ -CD.L.Zn was solely responsible for the increase in absorbance and the detectable color change of the stained yeast cells. Thus, these two reagents could be used as viable and efficient colorimetric staining agents for prokaryotic and eukaryotic microbes for viewing through optical microscope. Further, these reagents also could be used for studies on cell growth dynamics, which has relevance in terms of industrial application.

## CONCLUSION

Two colorimetric reagents, L.Zn and its [2]pseudorotaxane form ( $\alpha$ -CD.L.Zn), were used successfully for recognition and detection of ATP produced in situ during different metabolic processes in living organisms in pure aq HEPES buffer (pH = 7.2) medium. Lower detection limits, evaluated for these two reagents, were found to be much lower than the typical concentration of ATP in live cells of eukaryotic and prokaryotic microbes. Studies further revealed that both colorimetric reagents were nontoxic to the living microbes and could be used for staining live cells of respective microbes for viewing through light microscope. Experimental results confirmed that viability of the live cells of *Saccharomyces cerevisiae*, *Pseudomonas fluorescence*, and *Bacillus megaterium* was maintained in the presence of these two reagents and could be used for studying the cell growth dynamics of each of these individual microbes.

## ASSOCIATED CONTENT

**S Supporting Information.** Details regarding synthesis, characterization, solubility experiment, <sup>31</sup>P NMR study, spectrophotometric titrations, reversibility study, and interference study. Additional information as noted in text. This material is available free of charge via the Internet at <http://pubs.acs.org>.

## AUTHOR INFORMATION

### Corresponding Author

\*E-mail: [amitava@csmcri.org](mailto:amitava@csmcri.org) (A.D.).

## ACKNOWLEDGMENT

AD thanks DST (New Delhi) and CSIR (India) for financial support. PM, AG, SKM and AS acknowledge CSIR for their Sr. Research Fellowship.

## REFERENCES

- (1) (a) Gale, P. A. *Chem. Commun.* **2011**, 47, 82. (b) Wade, C. R.; Broomsgrove, A. E. J.; Aldridge, S.; Gabbai, F. P. *Chem. Rev.* **2010**, *110*, 3958. (c) Sinkeldam, R. W.; Greco, N. J.; Tor, Y. *Chem. Rev.* **2010**, *110*, 2579. (d) Quang, D. T.; Kim, J. S. *Chem. Rev.* **2010**, *110*, 6280. (e) Gale, P. A. *Chem. Soc. Rev.* **2010**, *39*, 3746. (f) Liu, J.; Cao, Z.; Lu, Y. *Chem. Rev.* **2009**, *109*, 1948. (g) Ba\_u, L.; Tecilla, P.; Mancin, F. *Nanoscale* **2010** in print. (h) Kim, H. N.; Guo, Z.; Zhu, W.; Yoon, J.; Tian, H. *Chem. Soc. Rev.* **2010** in press. (i) Qian, X.; Xiao, Y.; Xu, Y.; Guo, X.; Qiana, J.; Zhua, W. *Chem. Commun.* **2010**, 46, 6418. (j) Galbraith, E.; James, T. D. *Chem. Soc. Rev.* **2010**, *39*, 3831. (k) Chen, X.; Zhou, Y.; Peng, X.; Yoon, J. *Chem. Soc. Rev.* **2010**, *39*, 2120. (l) Xu, Z.; Yoon, J.; Spring, D. R. *Chem. Soc. Rev.* **2010**, *39*, 1996. (m) Zhao, Q.; Li, F.; Huang, C. *Chem. Soc. Rev.* **2010**, *39*, 3007. (n) Xu, Z.; Chen, X.; Kim, H. N.; Yoon, J. *Chem. Soc. Rev.* **2010**, *39*, 127. (o) Cametti, M.; Rissanen, K. *Chem. Commun.* **2009**, 2809. (p) Chen, X.; Kang, S.; Kim, M. J.; Kim, J.; Kim, Y. S.; Kim, H.; Chi, B.; Kim, S.-J.; Lee, J. Y.; Yoon, J. *Angew. Chem., Int. Ed.* **2010**, *49*, 1422. (q) Kou, S.; Lee, H. N.; van Noort, D.; Swamy, K. M. K.; Kim, S. H.; Soh, J. H.; Lee, K.-M.; Nam, S.-W.; Yoon, J.; Park, S. *Angew. Chem., Int. Ed.* **2008**, *47*, 872.
- (2) (a) Saha, S.; Ghosh, A.; Mahato, P.; Mishra, S.; Mishra, S. K.; Suresh, E.; Das, S.; Das, A. *Org. Lett.* **2010**, *12*, 3406. (b) Das, P.; Ghosh, A.; Das, A. *Inorg. Chem.* **2010**, *49*, 6909. (c) Ghosh, A.; Jose, D. A.; Das, A.; Ganguly, B. *J. Mol. Model.* **2010**, *16*, 1441. (d) Suresh, M.; Das, A. *Tetrahedron Lett.* **2009**, *50*, 5808. (e) Ghosh, A.; Verma, S.; Ganguly, B.; Ghosh, H. N.; Das, A. *Eur. J. Inorg. Chem.* **2009**, 2496. (f) Suresh, M.; Ghosh, A.; Das, A. *Chem. Commun.* **2008**, 3906. (g) Jose, D. A.; Kumar, D. K.; Kar, P.; Verma, S.; Ghosh, A.; Ganguly, B.; Ghosh, H. N.; Das, A. *Tetrahedron* **2007**, *63*, 12007. (h) Jose, D. A.; Singh, A.; Ganguly, B.; Das, A. *Tetrahedron Lett.* **2007**, *48*, 3695. (i) Ghosh, A.; Ganguly, B.; Das, A. *Inorg. Chem.* **2007**, *46*, 9912. (j) Kar, P.; Suresh, M.; Kumar, D. K.; Jose, D. A.; Ganguly, B.; Das, A. *Polyhedron* **2007**, *26*, 1317. (k) Jose, D. A.; Kumar, D. K.; Ganguly, B.; Das, A. *Inorg. Chem.* **2007**, *46*, 5817. (l) Jose, D. A.; Kar, P.; Koley, D.; Ganguly, B.; Thiel, W.; Ghosh, H. N.; Das, A. *Inorg. Chem.* **2007**, *46*, 5576. (m) Jose, D. A.; Kumar, D. K.; Ganguly, B.; Das, A. *Tetrahedron Lett.* **2005**, *46*, 5343. (n) Jose, D. A.; Kumar, D. K.; Ganguly, B.; Das, A. *Org. Lett.* **2004**, *6*, 3445.
- (3) (a) Mandal, A. K.; Suresh, M.; Suresh, E.; Mishra, S. K.; Mishra, S.; Das, A. *Sens. Actuators, B* **2010**, *145*, 32. (b) Suresh, M.; Mishra, S.; Mishra, S. K.; Suresh, E.; Mandal, A. K.; Shrivastav, A.; Das, A. *Org. Lett.* **2009**, *11*, 2740. (c) Suresh, M.; Shrivastav, A.; Mishra, S.; Suresh, E.; Das, A. *Org. Lett.* **2008**, *10*, 3013. (d) Suresh, M.; Mishra, S. K.; Mishra, S.; Das, A. *Chem. Commun.* **2009**, 2496. (e) Suresh, M.; Mandal, A. K.; Saha, S.; Suresh, E.; Mandoli, A.; Liddo, R. D.; Parnigotto, P. P.; Das, A. *Org. Lett.* **2010**, *12*, 5406. (f) Kurishita, Y.; Kohira, T.; Ojida, A.; Hamachi, I. *J. Am. Chem. Soc.* **2010**, *132*, 13290. (g) Lee, C.-H.; Miyaji, H.; Yoon, D.-W.; Sessler, J. L. *Chem. Commun.* **2008**, *1*, 24. (h) Gunnlaugsson, T.; Glynn, M.; Tocci, G. M.; Kruger, P. E.; Pfeffer, F. M. *Coord. Chem. Rev.* **2006**, *250*, 3094. (i) Martínez-Máñez, R.; Sancaón, F. *Chem. Rev.* **2003**, *103*, 4419. (j) Callan, J. F.; de Silva, A. P.; Magri, D. C. *Tetrahedron* **2005**, *61*, 8551. (k) Zhao, J.; Fyles, T. M.; James, T. D. *Angew. Chem., Int. Ed.* **2004**, *43*, 3461. (l) Gale, P. A. *Acc. Chem. Res.* **2006**, *39*, 465. (m) Kim, S. K.; Lee, D. H.; Hong, J.-I.; Yoon, J. *Acc. Chem. Res.* **2009**, *42*, 23. (n) Huang, X.; Guo, Z.; Zhu, W.; Xie, Y.; Tian, H. *Chem. Commun.* **2008**, 5143.
- (4) (a) Mahato, P.; Ghosh, A.; Saha, S.; Mishra, S.; Mishra, S. K.; Das, A. *Inorg. Chem.* **2010**, *49*, 11485. (b) Li, T.; Li, B.; Wang, E.; Dong, S. *Chem. Commun.* **2009**, 3551. (c) Sancenón, F.; Martínez-Manez, R.; Soto, J. *Tetrahedron Lett.* **2001**, *42*, 4321. (d) Choi, M. J.; Kim, M. Y.; Chang, S.-K. *Chem. Commun.* **2001**, 1664. (e) Sancenón, F.; Martínez-Manez, R.; Soto, J. *Chem. Commun.* **2001**, 2262. (f) Brummer, O.; La Clair, J. J.; Janda, K. D. *Org. Lett.* **1999**, *1*, 415.
- (5) (a) Coronado, E.; Galán-Mascarós, J. R.; Martí-Gastaldo, C.; Palomares, E.; Durrant, J. R.; Vilar, R.; Gratzel, M.; Nazeeruddin, M. K. *J. Am. Chem. Soc.* **2005**, *127*, 12351. (b) Lee, S.-H.; Kumar, J.; Tripathy, S. K. *Langmuir* **2000**, *16*, 10482. (c) Ren, X.; Xu, Q.-H. *Langmuir* **2009**, *25*, 29. (d) Hirayama, T.; Taki, M.; Kashiwagi, Y.; Nakamoto, M.; Kunishita, A.; Itoh, S.; Yamamoto, Y. *Dalton Trans.* **2008**, 4705. (e) Zhang, D.; Deng, M.; Xu, L.; Zhou, Y.; Yuwen, J.; Zhou, X. *Chem.—Eur. J.* **2009**, *15*, 8117. (f) Liu, X.; Tang, Y.; Wang, L.; Zhang, J.; Song, S.; Fan, C.; Wang, S. *Adv. Mater.* **2007**, *19*, 1471. (g) Lee, H.; Lee, S. S. *Org. Lett.* **2009**, *11*, 1393. (h) Zhou, Y.; Zhu, C.-Y.; Gao, X.-S.; You, X.-Y.; Yao, C. *Org. Lett.* **2010**, *12*, 2566.
- (6) (a) Xu, Z.; Kim, S. K.; Yoon, J. *Chem. Soc. Rev.* **2010**, *39*, 1457. (b) Sakaguchi, R.; Tainaka, K.; Shimada, N.; Nakano, S.; Inoue, M.; Kiyonaka, S.; Mori, Y.; Morii, T. *Angew. Chem., Int. Ed.* **2010**, *122*, 2196. (c) Cort, A. D.; Bernardin, P. D.; Forte, G.; Mihan, F. Y. *Chem. Soc. Rev.* **2010**, *39*, 3863. (d) Moro, A. J.; Cywinski, P. J.; Körstena, S.; Mohr, G. J. *Chem. Commun.* **2010**, 46, 1085. (e) Kwon, T.-H.; Kim, H. J.; Hong, J.-I. *Chem.—Eur. J.* **2008**, *14*, 9613. (f) Schmidt, F.; Stadlbauer, S.; König, B. *Dalton Trans.* **2010**, 39, 7250.
- (7) (a) García-España, E.; Díaz, P.; Llinares, J. M.; Bianchi, A. *Coord. Chem. Rev.* **2006**, *250*, 2952. (b) Duke, R. M.; O'Brien, J. E.; McCabe, T.; Gunnlaugsson, T. *Org. Biomol. Chem.* **2008**, *6*, 4089.
- (8) (a) Hunter, T. In *Protein Phosphorylation*; Sefton, B. M., Ed.; Academic Press, New York, 1998. (b) Pawson, T.; Scott, J. D. *Trends Biochem. Sci.* **2005**, *30*, 286. (c) Johnson, L. N.; Lewis, R. J. *Chem. Rev.* **2001**, *101*, 2209. (d) Yaffe, M. B. *Nat. Rev. Mol. Cell Biol.* **2002**, *3*, 177. (e) Yaffe, M. B.; Elia, A. E. H. *Curr. Opin. Cell Biol.* **2001**, *13*, 131. (f) Knowles, J. R. *Annu. Rev. Biochem.* **1980**, *49*, 877. (g) Mathews, C. P.; van Hold, K. E. *Biochemistry*; The Benjamin/Cummings Publishing Co. Inc.: Redwood City, CA, 1990. (h) Bush, K. T.; Keller, S. H.; Nigam, S. K. *J. Clin. Invest.* **2000**, *106*, 621. (i) Kim, S. K.; Lee, D. H.; Hong, J. I.; Yoon, J. *Acc. Chem. Res.* **2009**, *42*, 23.
- (9) (a) Tsujimoto, Y. *Cell Death Differ.* **1997**, *4*, 429. (b) Eguchi, Y.; Shimizu, S.; Tsujimoto, Y. *Cancer Res.* **1997**, *57*, 1835. (c) Takeda, E.; Yamamoto, H.; Nashiki, K.; Sato, T.; Arai, H.; Taketani, Y. *J. Cell. Mol. Med.* **2004**, *8*, 191.
- (10) (a) Bush, K. T.; Keller, S. H.; Nigam, S. K. *J. Clin. Invest.* **2000**, *106*, 621. (b) Przedborski, S.; Vila, M. *Clin. Neurosci. Res.* **2001**, *1*, 407. (c) Harkness, R. A.; Saugstad, O. D. *Scand. J. Clin. Lab. Invest.* **1997**, *57*, 655. (d) Faris, A.; Spence, D. M. *Analyst* **2008**, *133*, 678.
- (11) Ludin, A.; Hasenson, M.; Persson, J.; Pousette, A. *Methods Enzymol.* **1986**, *133*, 27.
- (12) *The Handbook: A Guide to Fluorescent Probes and Labeling Technologies*, 10th ed.; Invitrogen: Carlsbad, CA, 2005; Chapter 10–3.
- (13) (a) Zhang, X.; Zhao, Y.; Li, S.; Zhang, S. *Chem. Commun.* **2010**, 9173. (b) Berg, J.; Hung, Y.-P.; Yellen, G. *Nat. Methods* **2009**, *6*, 161. (c) Ruiz-Stewart, I.; Tiyyagura, S. R.; Lin, J. E.; Kazerounian, S.; Pitari, G. M.; Schulz, S.; Martin, E.; Murad, F.; Waldman, S. A. *Proc. Natl. Acad. Sci. U.S.A.* **2004**, *101*, 37. (d) Nikolaev, V. O.; Gambaryan, S.; Lohse, M. J. *Nat. Methods* **2006**, *3*, 23. (e) Sato, M.; Ozawa, T.; Inukai, K.; Asano, T.; Umezawa, Y. *Nat. Biotechnol.* **2002**, *20*, 287. (f) Ting, A. Y.; Kain, K. H.; Klemke, R. L.; Tsien, R. Y. *Proc. Natl. Acad. Sci. U.S.A.* **2001**, *98*, 15003. (g) Zhang, J.; Ma, Y.; Taylor, S. S.; Tsien, R. Y. *Proc. Natl. Acad. Sci. U.S.A.* **2001**, *98*, 14997. (h) Zuo, X.; Song, S.; Zhang, J.; Pan, D.; Wang, L.; Fan, C. *J. Am. Chem. Soc.* **2007**, *129*, 1042.
- (14) (a) Li, D.; Song, S.; Fan, C. *Acc. Chem. Res.* **2010**, *43*, 631. (b) Zhang, H.; Fang, C.; Zhang, S. *Chem.—Eur. J.* **2010**, *16*, 12434. (c) Laudet, E.; Hatz, S.; Droniou, M.; Dale, N. *Anal. Chem.* **2005**, *77*, 3267. (d) Lloris, J. M.; Martínez-Máñez, R.; Padilla-Tosta, M. E.; Pardo, T.; Soto, J.; García-España, E.; Ramírez, J. A.; Burguete, M. I.; Luis, S. V.; Sinn, E. *J. Chem. Soc., Dalton Trans.* **1999**, 1779. (e) Bücking, W.; Urban, G. A.; Nanna, T. *Sens. Actuators, B* **2005**, *104*, 111. (f) Zuo, X.; Song, S.; Zhang, J.; Pan, D.; Wang, L.; Fan, C. *J. Am. Chem. Soc.* **2007**, *129*, 1042.
- (15) (a) Xu, Z.; Kim, S. K.; Yoon, J. *Chem. Soc. Rev.* **2010**, *39*, 1457. (b) Xu, Z.; Singh, N. J.; Lim, J.; Pan, J.; Kim, H. N.; Park, S.; Kim, K. S.; Yoon, J. *J. Am. Chem. Soc.* **2009**, *131*, 15528. (c) Sakamoto, T.; Ojida, A.; Hamachi, I. *Chem. Commun.* **2009**, 141 and references therein. (d) Rhee, H.-W.; Lee, C.-R.; Cho, S.-H.; Song, M.-R.; Cashel, M.; Choy, H. E.; Seok, Y.-J.; Hong, J.-I. *J. Am. Chem. Soc.* **2008**, *130*, 784. (e) Zeng, Z.; Torriero, A. A. J.; Bond, A. M.; Spiccia, L. *Chem.—Eur. J.* **2010**, *16*, 9154. (f) Schäferling, M.; Wolfbeis, O. S. *Chem.—Eur. J.* **2007**, *13*, 4342. (g) Jose, D. A.; Stadlbauer, S.; König, B. *Chem.—Eur. J.* **2009**, *15*, 7404. (h)



- Mizukami, S.; Nagano, T.; Urano, Y.; Odani, Y.; Kikuchi, K. *J. Am. Chem. Soc.* **2002**, *124*, 3920. (i) Ojida, A.; Nonaka, H.; Miyahara, Y.; Tamaru, S.-i.; Sada, K.; Hamachi, I. *Angew. Chem., Int. Ed.* **2006**, *45*, 5518. (j) O'Neil, E. J.; Smith, B. D. *Coord. Chem. Rev.* **2006**, *250*, 3068. (k) Wang, H.; Chan, W.-H. *Org. Biomol. Chem.* **2008**, *6*, 162. (l) Ojida, A.; Takashima, I.; Kohira, T.; Nonaka, H.; Hamachi, I. *J. Am. Chem. Soc.* **2008**, *130*, 12095. (m) Ojida, A.; Miyahara, Y.; Wongkongkatap, J.; Tamaru, S.-i.; Sada, K.; Hamachi, I. *Chem.—Asian J.* **2006**, *1*, 555. (n) Florea, M.; Nau, W. M. *Org. Biomol. Chem.* **2010**, *8*, 1033. (o) An, L.; Tang, Y.; Feng, F.; He, F.; Wang, S. *J. Mater. Chem.* **2007**, *17*, 4147. (p) Jang, H. H.; Yi, S.; Kim, M. H.; Kim, S.; Lee, N. H.; Han, M. S. *Tetrahedron Lett.* **2009**, *50*, 6241.
- (16) (a) Wang, J.; Wang, L.; Liu, X.; Liang, Z.; Song, S.; Li, W.; Li, G.; Fan, C. *Adv. Mater.* **2007**, *19*, 3943. (b) Buryak, A.; Zaubitzer, F.; Pozdnoukhov, A.; Severin, K. *J. Am. Chem. Soc.* **2008**, *130*, 11260. (c) Chen, S.-J.; Huang, Y.-F.; Huang, C.-C.; Lee, K.-H.; Lin, Z.-H.; Chang, H.-T. *Biosens. Bioelectron.* **2008**, *23*, 1749. (d) McCleskey, S. C.; Griffin, M. J.; Schneider, S. E.; McDevitt, J. T.; Anslyn, E. V. *J. Am. Chem. Soc.* **2003**, *125*, 1114. (e) Ishida, A.; Yamada, Y.; Kamidate, T. *Anal. Bioanal. Chem.* **2008**, *392*, 987. (f) Sancenón, F.; Descalzo, A. B.; Martínez-Mañiz, R.; Miranda, M. A.; Soto, J. *Angew. Chem., Int. Ed.* **2001**, *40*, 2640. (g) Li, C.; Numata, M.; Takeuchi, M.; Shinkai, S. *Angew. Chem., Int. Ed.* **2005**, *44*, 6371. (h) Buryak, A.; Pozdnoukhov, A.; Severin, K. *Chem. Commun.* **2007**, 2366. (i) Ma, T.; Li, C.; Shi, G. *Langmuir* **2008**, *24*, 43.
- (17) (a) Mahato, P.; Ghosh, A.; Mishra, S. K.; Shrivastav, A.; Mishra, S.; Das, A. *Chem. Commun.* **2010**, 9134. (b) Ghosh, A.; Shrivastav, A.; Jose, D. A.; Mishra, S. K.; Chandrakanth, C. K.; Mishra, S.; Das, A. *Anal. Chem.* **2008**, *80*, 5312. (c) Jose, D. A.; Mishra, S.; Ghosh, A.; Shrivastav, A.; Mishra, S. K.; Das, A. *Org. Lett.* **2007**, *9*, 1979.
- (18) Lim, D. *Microbiology*, 2nd ed.; William C. Brown/McGraw Hill: New York, 1998.
- (19) (a) Nelson, D. A.; Cox, M. M.; Lehninger, A. *Principles of Biochemistry*, 4th ed.; W.H. Freeman and Co.: New York, 2006. (b) Bergey, D. H.; John, G. H.; Noel, R. K.; Peter, H. A. S. *Bergey's Manual of Determinative Bacteriology*, 9th ed.; Lippincott Williams & Wilkins: Philadelphia, 1994.
- (20) Bergey, D. H.; Holt, J. G.; Krieg, N. R.; Sneath, P. H. A. *Bergey's Manual of Determinative Bacteriology*, 9th ed.; Lippincott Williams & Wilkins: Philadelphia, 1994.
- (21) Cahill, G.; Walsh, P. K.; Donnelly, D. *J. Am. Soc. Brew. Chem.* **1999**, *57*, 72.
- (22) Zhang, T.; Fang, H. H. P. *Biotechnol. Lett.* **2004**, *26*, 989.
- (23) (a) Biswas, K.; Rieger, K.; Morschhäuser, J. *Gene* **2003**, *307*, 151. (b) Dan, N. P.; Visvanathan, C.; Basu, B. *Bioresour. Technol.* **2003**, *87*, 51.
- (24) Millsap, K. W.; van der Mei, H. C.; Bos, R.; Busscher, H. J. *FEMS Microbiol. Rev.* **1998**, *21*, 321.
- (25) (a) Narvhus, J. A.; Gadaga, T. H. *Int. J. Food Microbiol.* **2003**, *86*, 51. *S. cerevisiae* is the most commonly used species in the brewing and production of ethanol in the industry where quality control is required for consistent production and where such chemical sensors could be utilized to monitor the biological growth and also check the viability of the cells therein. The biological processes involved therein are unpredictable, so they need to be monitored at regular intervals.
- (26) Baskin, D. S.; Ngo, H.; Didenko, V. V. *Toxicol. Sci.* **2003**, *74*, 361.
- (27) Valeur, B.; Pouget, J.; Bouson, J. *J. Phys. Chem.* **1992**, *96*, 6545.
- (28) (a) Benesi, H. A.; Hildebrand, J. H. *J. Am. Chem. Soc.* **1949**, *71*, 2703. (b) Yang, C.; Liu, L.; Mu, T.-W.; Guo, Q.-X. *Anal. Sci.* **2000**, *16*, 537. (c) Rodríguez-Cáceres, M. I.; Agbaria, R. A.; Warner, I. M. *J. Fluoresc.* **2005**, *15*, 185.
- (29) (a) Lindloy, L. F.; Busch, D. H. *Inorg. Chem.* **1974**, *13*, 2494. (b) Wester, D.; Palenik, G. J. *J. Am. Chem. Soc.* **1974**, *95*, 6505.
- (30) Horton, H. R.; Moran, L. A.; Scrimgeour, K. G.; Perry, M. D.; Rawn, J. D. *Principles of Biochemistry*; Prentice Hall: Upper Saddle River, NJ, 2006.
- (31) (a) Wenz, G. J.; Han, B.-H.; Muller, A. *Chem. Rev.* **2006**, *106*, 782. (b) Wylie, R. S.; Macartney, D. H. *Inorg. Chem.* **1993**, *32*, 1830. (c) Baer, A. J.; Macartney, D. H. *Inorg. Chem.* **2000**, *39*, 1410. (d) Wenz, G. *Angew. Chem., Int. Ed. Engl.* **1994**, *33*, 803. (e) Sanchez, A. M.; de Rossi, R. H. *J. Org. Chem.* **1996**, *61*, 3446. (f) Liu, Y.; Zhao, Y.-L.; Chen, Y.; Guo, D.-S. *Org. Biomol. Chem.* **2005**, *3*, 584. (g) Zhang, X.; Gramlich, G.; Wang, X.; Nau, W. M. *J. Am. Chem. Soc.* **2002**, *124*, 254. (h) Macartney, D. H.; Wadding, C. A. *Inorg. Chem.* **1994**, *33*, 5912. (i) Smith, A. C.; Macartney, D. H. *J. Org. Chem.* **1998**, *63*, 9243. (j) Abou-Hamdan, A.; Bugnon, P.; Saudan, C.; Lye, P. G.; Merbach, A. E. *J. Am. Chem. Soc.* **2000**, *122*, 592. (k) Yamamoto, Y.; Kanda, Y.; Inoue, Y.; Chujo, R.; Kobayashi, S. *Chem. Lett.* **1988**, 495. (l) Steefkerk, D. G.; De Bie, M. J. A.; Vliegthart, J. F. G. *Tetrahedron* **1973**, *29*, 833. (m) Liu, Y.; Zhao, Y.-L.; Chen, Y.; Guo, D.-S. *Org. Biomol. Chem.* **2005**, *3*, 584. (n) Bratu, I.; Gavira-Vallejo, J. M.; Hernanz, A. *Biopolymers* **2005**, *77*, 361. (o) Fonza, G.; Mele, A.; Redenti, E.; Ventura, P. *J. Org. Chem.* **1996**, *61*, 909. (p) Pérez-Martínez, J. I.; Ginés, J. M.; Morillo, E.; Moyano, J. R. *J. Inclusion Phenom. Macrocyclic Chem.* **2000**, *37*, 171.
- (32) (a) Shukla, A. D.; Bajaj, H. C.; Das, A. *Angew. Chem., Int. Ed.* **2001**, *40*, 446. (b) Shukla, A. D.; Bajaj, H. C.; Das, A. *Proc. Indian Acad. Sci., Chem. Sci.* **2002**, *114*, 431.
- (33) (a) Connors, K. A. *Chem. Rev.* **1997**, *97*, 1325 and references therein. (b) Nepogodiev, S. A.; Stoddart, J. F. *Chem. Rev.* **1998**, *98*, 1959.
- (c) Siddarth, P.; Marcus, R. A. *J. Phys. Chem.* **1990**, *94*, 2985.
- (34) Durette, L.; Horton, D. *Org. Magn. Reson.* **1971**, *3*, 417.
- (35) Ivanova, E. P.; Alexeeva, Y. V.; Pham, D. K.; Wright, J. P.; Nicolau, D. V. *Int. Microbiol.* **2006**, *9*, 37.
- (36) Beveridge, T. J. *J. Bacteriol.* **1999**, *181*, 4725.
- (37) Beis, I.; Newsholme, E. A. *J. Biochem.* **1975**, *152*, 23.
- (38) (a) Nakashima, H. *Plant Physiol.* **1984**, *76*, 612. (b) Li, N.; Ragheb, K.; Lawler, G.; Sturgis, J.; Rajwa, B.; Melendez, A.; Robinson, J. P. *J. Biol. Chem.* **2003**, *278*, 8516. (c) Gbelska, Y.; Julius, S.; Svoboda, A.; Goffeau, A.; Kovac, L. *Eur. J. Biochem.* **1983**, *130*, 281.
- (39) Wada, M.; Kogure, K.; Ohwada, K.; Simidu, U. *J. Gen. Microbiol.* **1992**, *138*, 2525.
- (40) Gao, H. M.; Liu, B.; Hong, J. S. *J. Neurosci.* **2003**, *23*, 6181.